ON TRANSVERSE FRACTURE MECHANISMS OF 1140+/Ti-6Al-4V AND SCS-6/Ti ß21S COMPOSITES UNDER TENSILE LOADING

X. Wu (1), H.Mori (2) and P. Bowen (1)

1 School of Metallurgy and Materials, The University of Birmingham, Edgbaston, Birmingham, B15 2TT, UK
2 Research Centre for Advanced Science and Technology, The University of Tokyo, 4-6-1 Komaba, Meguro-ku, Tokyo 153, Japan

SUMMARY: The transverse behaviour of 1140+/Ti-6Al-4V and SCS-6/Ti ß21s composites has been investigated by tensile tests in air and in situ within a FEG-SEM using direct observations. Acoustic Emission Analysis(AE) has also been used to assess and locate positions of damage. It has been observed that debonding in both composites can start at very low stresses due to defects and/or undulations at interfaces. AE events can be found almost immediately on loading during premature debonding of SCS-6/Ti ß21s, but few for the 1140+/Ti-6-4 composite. Many AE events of high energies were detected in the region of the first knee on stress ~ time curves. The peak energies of AE obtained in 1104+/Ti-6-4 and SCS-6/Ti ß21s are of ~150 and ~650µJ, respectively. Cracking of carbon coatings and/or reaction zones also produce distinct AE events. Distinct differences in AE behaviour have been found between 1140+/Ti-6-4 and SCS-6/Ti ß21s composites.

KEYWORDS: transverse tensile loading, AE behaviour, in situ observation, debonding.

INTRODUCTION

During the last decade extensive research has been carrying out on unidirectional fibre re-inforced titanium matrix composites, due to their potential applications in aerospace. Recently transverse properties are also among of interest not least because transverse damage can be present in cracked testpieces even when the applied stress is along the longitudinal direction alone[1]. Since fibre reinforcement gives potential sites of weakness in such transverse directions, the introduction of significant transverse stresses can be a problem. It has been suggested[2] that the transverse stress *versus* strain curve can be classified into five regions, and each region marks an individual process at a given stress range. For example, the first linear region is attributed to elastic deformation of the composite, and a distinct first "knee" is attributed to debonding of the fibre/ matrix interface. In the SCS-6/Ti-6-4 composite it has been seen that debonding of un-coated single fibre/matrix interfaces can occur at lower stresses due to defects at the interface induced by incomplete consolidation[3].

A range of stresses has also been obtained for individual fibres rather than a single value which is often quoted. This study reports a thorough investigation of the dynamic mechanisms in composites during tensile loading by in situ observations in a FEG-SEM, which allows the entire dynamic process during loading to be directly monitored, filmed and recorded. Conventional tensile tests were also used, assisted by an acoustic emission(AE) system to provide information on damage. The materials studied here are Sigma 1140+/Ti-6-4 and SCS-6/Ti ß21s TiMMCs. Those MMCs have been considered to possess lower and higher fibre/matrix interface bonding strengths[4], respectively.

EXPERIMENTAL PROCEDURE

The composites studied here are 8 and 21%1140+/Ti-6-4 and 35%SCS-6/Ti ß21s. The 1140+/Ti-6-4 composites were received in the form of a 12-ply plate with thickness of ~3.5 mm and an 8-ply plate with thickness of ~1.82 mm, for the 8 and 21% fibre volume fraction composites, respectively. The 35% SCS-6/Ti ß21s plate was also an 8-ply plate with a thickness of approximately 1.8 mm. The chemical composition of the Ti ß21s is: 15Mo, 2.7Nb, 3Al, and 0.2Si(wt.%). These plates were then machined by using electro-discharge-machining(EDM) to produce conventional transverse tensile testpieces of length ~180 mm and width ~4 mm and *in situ* transverse testpieces of length ~80 mm and width ~2.5 mm. The distributions of fibres in transverse sections are shown in Fig. 1.

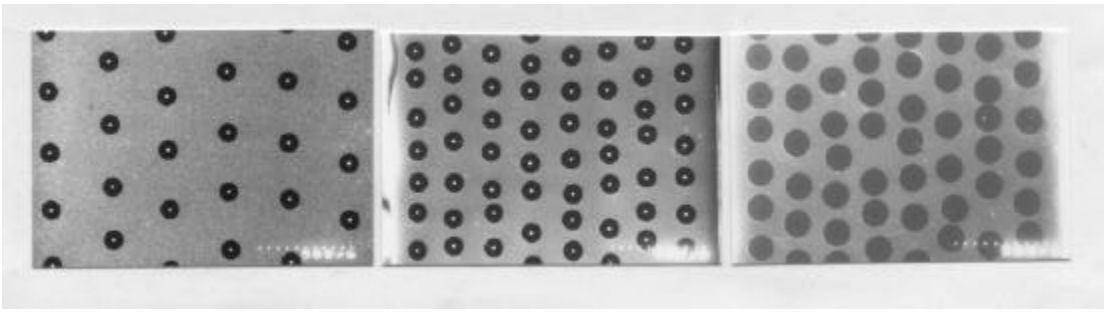

(a) (b) (c)

Fig. 1: Transverse sections of the composites: (a) 8% 1140+/Ti-6-4; (b) 21% 1140+/Ti-6-4 and (c) 35% SCS-6/Ti ß21s.

Conventional tensile tests were carried out on a 50kN Dartec M1000/RE servo-hydraulic testing machine. The testpieces were gripped hydraulically at each end between serrated plates which exerted a pressure of approximately 13 MPa. The gripped sections on a testpiece were tabbed by 1 mm thick aluminium strips on both sides using high strength, non-flowing adhesive Araldite(AV119)(cured at a temperature of 170 °C for 1 hour) in order to reduce damage from the grips and to facilitate failure within the gauge length. The gauge length is of ~50 mm for SCS-6/Ti ß21s and ~60 mm for 1140+/Ti-6-4 specimens. All conventional tensile tests were carried out under position control and at a ramp rate of 0.2 mm/min(i.e. ~3.3 µm/sec). Load, actuator displacement and time during testing were all recorded and analysized in detail.

AE signals from conventional tensile tests were detected by using two MICRO-100 sensors(PAC), which have capability to detect signals of frequency of up to 1000 kHz. Two sensors were glued on both ends of the gauge section at side surface of each testpiece, see Fig. 1, using a cyanoacrylate adhesive. A LOCAN320 AE system was used. Some upgrading

on the original AE software was made to allow location of AE signals by using two sensors, and therefore signals(noise) generated outside of the selected gauge length can be eliminated from the analysis.

In-situ tensile testing was conducted in an Hitachi S-4000 scanning electron microscope. The SEM was equipped with a Raith 10kN servoelectric screw driven loading stage capable of monotonic and cyclic loading. A suitable specimen configuration was devised for the in-situ loading stage. Strips of material of approximately 88mm length and 1.5 to 2mm width were cut from the TiMMC plates in the transverse direction using EDM. One transverse face of the strips was metallographically prepared to a 1µm diamond finish for observation in the SEM. Each end of these strips was adhesively bonded into a close fitting centre hole in a threaded stainless steel rod of 33mm length using araldite(AV119) epoxy, which required subsequent curing for 1 hour at 170 ^{o}C. This gave an observable gauge length of approximately 15mm. The threads were suitable for direct fitting into the loading stage crosshead adapter and load cell and the adhesive could sustain loads in excess of 3kN.

Testing was conducted at a crosshead speed of 2µm/sec, which compares well with the higher rate of 3.3µm/sec utilised for conventional testing in air. High resolution photographic images were obtained from the SEM at points of interest by interrupting the loading sequence and most of tests were interrupted at increments of 100 N(25~35 MPa). A continuous record of the tests was also made using a superVHS video recorder. The loading profile was recorded from the loading stage controllers onto analogue load and crosshead displacement outputs using an x-y plotter.

RESULTS

The tensile test results and some AE information obtained from 8 and 21%1140+/Ti-6-4 and 35%SCS-6/Ti ß21s MMCs are displayed in Figs. 2-5. The level of stress is indicated on the left-hand ordinate axis and the scale for AE parameters is indicated on the right-hand ordinate. The abscissa(time) is necessary to facilitate matching AE events to applied stresses. The transverse stress ~ strain responses of a range of 1140+/Ti-6-4 and SCS-6/Ti ß21s composites have been examined before[2, 5, 6] and the characteristics of the stress ~ strain curve is similar to that seen on the stress *versus* time curve in this study, Fig. 3. Thus the dynamic mechanisms are discussed in terms of applied stress level .

Figure 2 shows the results obtained from the 8% 1140+/Ti-6-4 composite. A linear increase of stress with time is first seen after loading starts (region I). At a stress of approximately 350 MPa, a slight change of gradient takes place, as arrowed, which produces the first "knee" on the curve (region II) and it is followed by a second linear period (region III), within which a slight change of gradient is also noted at ~520MPa, see double arrows. A second distinct further non-linearity on the stress~time curve occurs at ~720MPa (region IV), and afterwards the stress increases little before final catastrophic failure at a stress of 830 MPa(region V). Similarly five regions can also be identified on the stress ~ strain curve of the material, Fig. 3.

The cumulative AE events(dashed line) and the energy distribution of AE events(open squares) during the test are also displayed in Fig. 2. It can be seen that no AE events have been detected in the region I. A burst of AE events takes place spontaneously as the curve starts to deviate from linearity. These AE events have the highest energy, a maximum of ~150µJ, and this is approximately four times higher than other AE events(<30µJ). During the second linear period, a smaller second burst of AE events(<30µJ) was observed. Over the second "knee" and most of region V, AE events were infrequent until approaching the

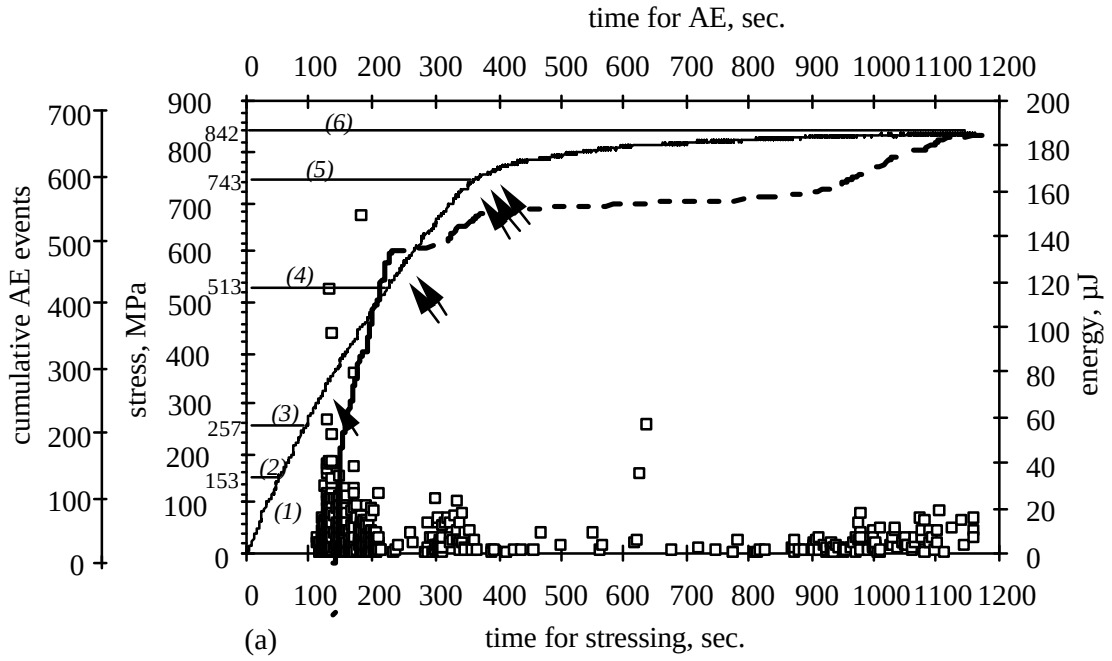

Fig. 2: Plots of stress vs time(solid line), cumulative AE events vs time(dashed line) and energies of AE events vs time(open squares) of the 8%1140+/Ti-6-4 under a conventional tensile test in air. Some in situ observation results(tested in the SEM) are also indicated by (1)-(6): (1) premature debonding due to defects and undulations; (2) 153 MPa, beginning of micro-debonding at the "perfect" carbon/carbon interfaces; (3) 257 MPa, fully debonding of all interfaces in the SEM; (4) 513 MPa, cracking of the reaction zone and carbon coating; (5) 743 MPa, multiple cracking of the carbon and reaction zone at the interfaces; and (6) 842 MPa, catastrophic failure of the in situ testpiece tested in the SEM.

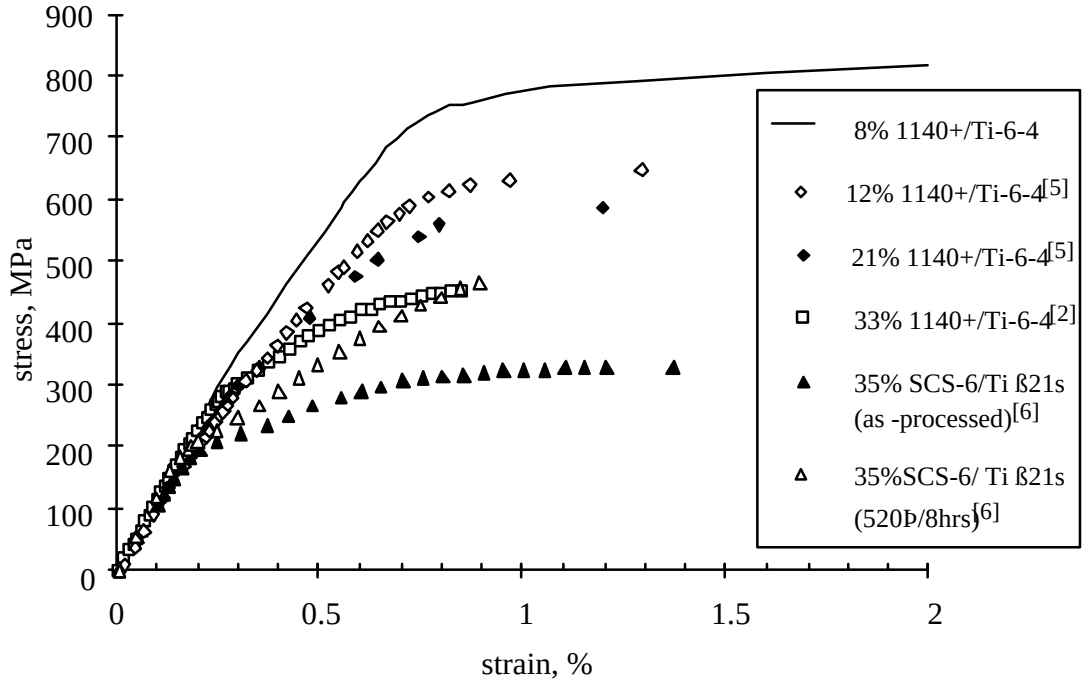

Fig. 3: Stress versus strain curves of various conditions of 1140+/Ti-6-4 and SCS-6/Ti ß21s composites under tensile loading.

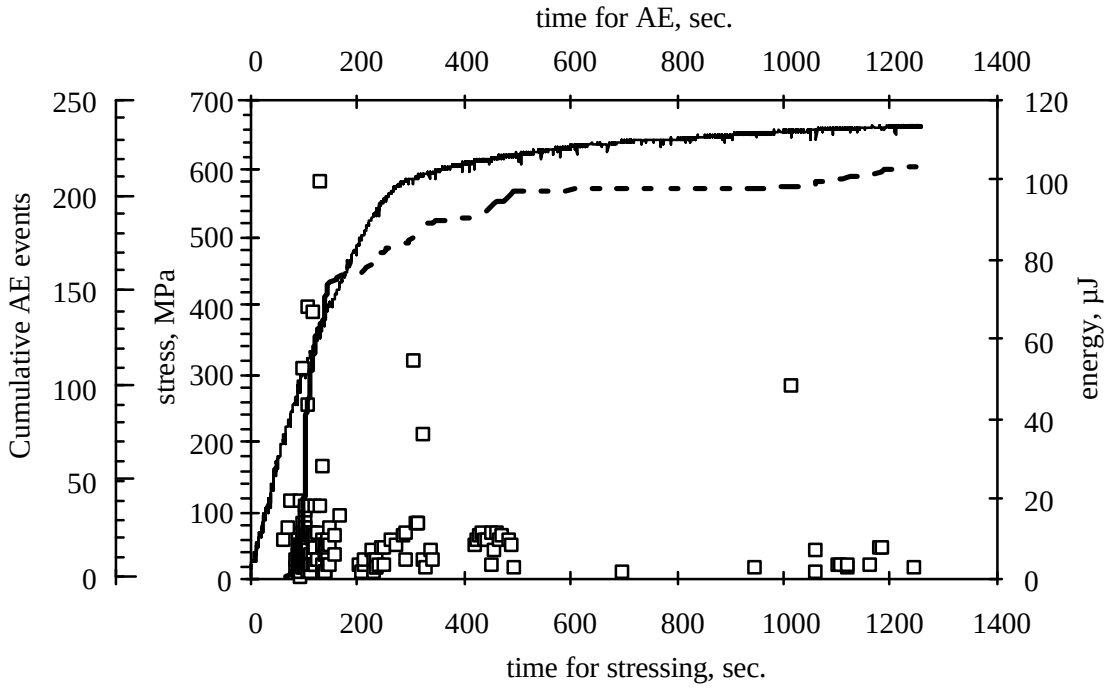

Fig. 4: Plots of stress vs time(solid line), cumulative AE events vs time(dashed line) and energies of AE events versus time(open squares) obtained from the 21% 1140+/Ti-6-4 composite under a conventional tensile test in air.

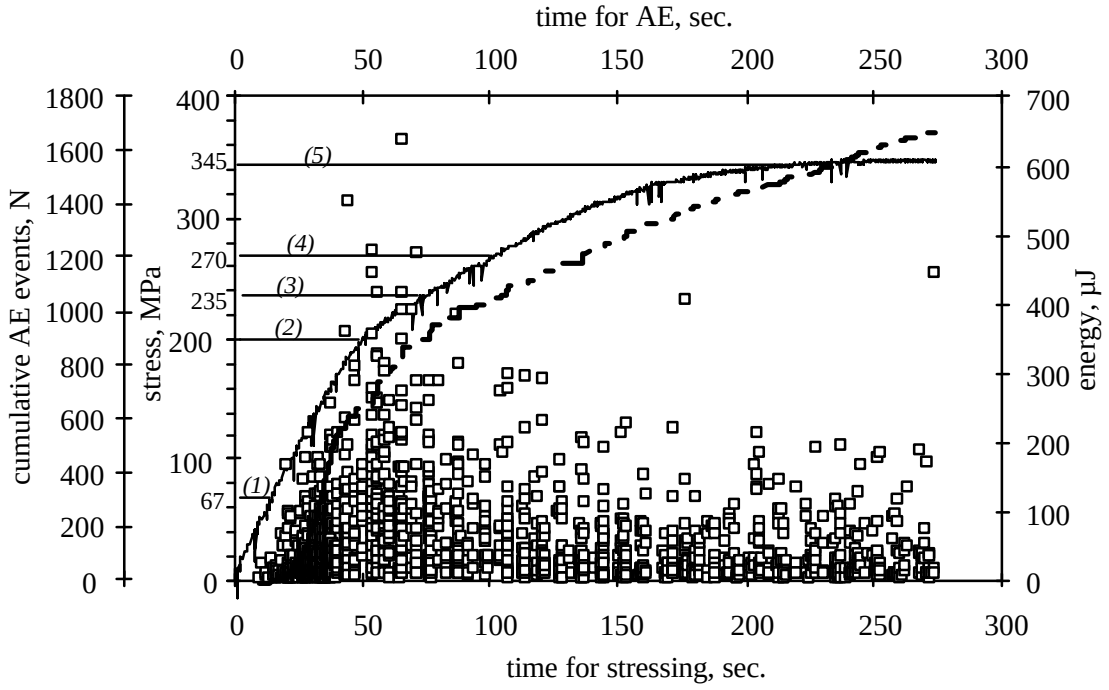

Fig. 5: Plots of stress vs time(solid line), cumulative AE events vs time(dashed line) and the energies of AE events vs time of the 35% SCS-6/Ti ß21s under a tensile test in air. Some in situ observation results(tested in the SEM) are also indicated by (1)-(5): (1) 67 MPa, premature micro-debonding due to defects; (2) 201 MPa, full debonding of all interfaces; (3) 235 MPa, multiple cracking in the reaction zone; (4) 270 MPa, occurrence of slip bands in the bulk matrix and (5) 345 MPa, catastrophic failure of the in situ testpiece.

final failure of the specimen, where many AE events were again noted. The number of AE events occurring at different regions are highlighted by the cumulative AE events curve(dashed line), Fig. 2. A dramatic increase of AE events is evident at the first knee.

The results obtained from the 21% 1140+/Ti-6-4 composite are shown in Fig. 4, which are very similar to that seen in the 8% 1140+/Ti-6-4 composite. The second knee on the stress~time curve of the 21% 1140+/Ti-6-4 composite occurs at a lower stress of ~600 MPa(compared with ~720 MPa in the 8% 1140+/Ti-6-4 composite). Bursts of AE events were again seen at both "knees" and limited counts were scattered throughout the rest of the period. The characteristics of AE events appears to be very similar in both composites.

Figure 5 shows the results obtained from the 35%SCS-6/Ti ß21s composite. The differences are obvious, compare with Figs. 2 and 4. A radical change of gradient at the first "knee" is now seen on the stress~time curve. It is also of interest to see in this material that AE events have been received almost immediately on loading, Fig. 5. Many AE events are now present in the linear region I. Note that the energy of the AE events increases with the increase of the applied stress, Fig. 5. The number of AE events is approximately five times higher in the 35%SCS-6/Ti ß21s composite, compare Figs. 5 and 2. It is also noted that the energy range in the SCS-6/Ti ß21s is much larger than that in the 1140+/Ti-6-4 composites. The peak energy of the AE events at the first knee now reaches ~650 μJ. AE events obtained in the regions of III, IV and V are also much more numerous than those obtained in 1140+/Ti-6-4 composites and they have an energy range of ~300 μJ, Fig. 5, which is approximately half of its peak energy at the first knee(~650 μJ). However this value is still approximately ten times higher than energies seen over the similar regions in the 1140+/Ti-6-4 composites(< 30μJ), Figs. 2 and 4.

DISCUSSION

The initial linear region I on a transverse tensile stress~strain (or time) has been previously suggested to be associated with elastic deformation of the composites and the first non-linearity is caused by debonding of fibre/matrix interfaces[2,3]. *In situ* observations in the FEG-SEM have found the detail is more complicated and a brief summary is given below (further details are reported elsewhere[7, 8]).

It has been found that debonding in 8 and 21%1140+/Ti-6-4 composites takes place primarily at the interface of carbon/carbon coating sublayer. If defects at the interface of carbon/reaction zone are severe, debonding can also take place at carbon/reaction zone interfaces. Micro-debonding appears at very low stresses from numerous locations due to sharp changes of curvature at the periphery of carbon/carbon interfaces or defects at carbon/reaction zone interfaces, regardless of the predicted location of maximum stress. The majority of "perfect" carbon/carbon interfaces are observed to initiate microcracks at a stress level of ~153 MPa and the effects of the position of maximum stress now appear to apply. The top and bottom of the interfaces are seen to be fully open at surface positions at a stress of approximately 260MPa for both 8 and 21% 1140+/Ti-6-4 composites. It is noted that no distinct change of gradient on stress~strain (or time) curves occurred during debonding below the stress of ~260MPa. The deviation from linearity on the stress~time curves starts under further loading after full surface debonding has already been observed in the SEM. After debonding, the reaction zone and the outermost carbon sublayer(first at θ=0, i.e. perpendicular to stress axis) has been observed to crack, whereas the major bulk matrix is still enduring elastic deformation only, at the stress of approximately 513 and 470 MPa in the 8 and 21% 1140+/Ti-6-4, respectively. During further loading those micro-cracks in the

reaction zone tend to be blunted by the un-reacted bulk matrix and arrested. Local plastic deformation at the two corners of the blunted crack tip was then induced, followed by gross plastic deformation of the matrix at the second knee. Further deformation leads to initiation of microcracks at the intruders of some favoured slip bands and catastrophic failure of the specimen by decohesion of the slip bands.

In the SCS-6/Ti ß21s composite, considerable micro-defects have also been seen, but now at the interface of carbon/reaction zone and these defects lead to earlier initiation of microcracks at very low stresses at the periphery of interfaces. Propagation and coalescence of these microcracks results in full debonding of those "imperfect" carbon/reaction zone interfaces at a stress of ~200 MPa within the SEM. It is noted that debonding in the SCS-6/Ti ß21s composite takes place at the interface of carbon/reaction zone, whereas in the 1140+/Ti-6-4 composite it mainly occurs at the carbon/carbon interface. In the SCS-6/Ti ß21s composite, distinct changes of gradient on stress~time curves have also been found to be simultaneous with full debonding seen in the SEM. Carbon layers at the interface of the SCS-6/Ti ß21s composite were seen to remain intact throughout the entire test, but microcracking of the reaction zone starts shortly after the first "knee" and it continues along the periphery of the interface until the final failure of the specimen. Those cracks were constrained within the reaction zone and blunted by the un-reacted matrix. Local plastic deformation is followed at the two corners of those blunted crack tips. In the 35%SCS-6/Ti ß21s the gross plastic deformation of the matrix is more localized and concentrated, with slip bands across the full width of a ligament.

A fibre/matrix interface there are two possible intrinsic stresses to overcome in order to achieve debonding: radial thermal residual stress(due to a mismatch of the thermal expansion coefficients of fibre and matrix) and chemical bonding stresses. The thermal residual stress makes the matrix physically clamp onto the fibre. Once the applied stress exceeds the thermal residual stress, the interface is then expected to separate if there is no any chemical bonding at the interface, in which case few AE events would be expected.

Figures 2 and 4 show that for 8 and 21% 1140+/Ti-6-4 composites no AE events have been detected in the linear region (I), i.e. the observed period of premature debonding. A burst of AE events(with energy of ~150 µJ) occur at the first knee where debonding on the surface has been seen to be complete at surface positions.

For the 35%SCS-6/Ti ß21s composite, premature debonding also starts from very low stresses due to defects. Fig. 5 shows that AE events can now be received during premature debonding in the first linear region. The AE events with a peak energy again occurs at the first knee, but now with a maximum energy of ~650 µJ.

As observed, debonding in the 35%SCS-6/Ti ß21s takes place at the carbon/reaction zone interface where intrinsic chemical bonding is assumed, whereas in the 1140+/Ti-6-4 debonding mainly takes place at the carbon/carbon sublayer interface. According to the different AE events in the linear region, it can be suggested that the chemical bonding strength is much higher at the debonded carbon/reaction zone interface in the 35%SCS-6/Ti ß21s than that at the debonded carbon/carbon interface in the 1140+/Ti-6-4 composite. In the latter composite any AE events from debonding in the linear region are too weak to be detected.

Figures 2 and 4 have shown a burst of AE events at the first "knee" with the highest energy (and amplitude), where the interface on the surface has already been seen to be fully open under *in situ* observations. As known during transverse tensile testing, the surface material is under two dimensional plane stress and inside the test piece is under three dimensional plane strain. A higher effective strain is obtained at the surface, which decreases towards the depth of interface tubes. Therefore it can be expected that the three-dimensional

interfacial debonding will take place at a higher applied stress than that for surface debonding. A burst of AE events at the first knee indicates that debonding or cracking is indeed taking place in the testpiece although it cannot be seen on the surface.

Combining the above discussion and in situ observation results, it can be deduced that interfacial debonding in 1140+/Ti-6-4 composites is an incremental process, starting from the surface at lower stresses and forming a ring crack. This ring crack then penetrates into the test piece along the interface "tube" at higher stresses. This appears to define the "first knee" primarily, as indicated by AE results. Figs 2 and 4 show that the peak energy region of AE events covers a stress range of 280 to 480 MPa in the 8% and 260 to 400 MPa in the 21% 1140+/Ti-6-4 composite, which gives an average stress for the first "knee" of 380 and 330 MPa respectively. Although the final stress for debonding may be affected by the thickness of a test piece(and chemical bonding strength, if it is significant), the initial debonding stress, here 280 MPa in the 8% 1140+/Ti-6-4 and 260 MPa in the 21% 1140+/Ti-6-4 composite is consistent with higher and lower thermal residual stresses in each composite, respectively.

From the stress~strain curves of 8, 21 and 33%1140+/Ti-6-4 composite (Fig. 3) it can be seen that differences between 21 and 33% are unclear. However the average stress for the first "knee" of the 8% 1140+/Ti-6-4 is higher. An analytical result of thermal residual stress by finite element method from a previous study[9] has found that an increase of fibre volume fraction may actually lead to a decrease of thermal residual stress(for a given type of fibre distribution pattern). However the scale in reduction of residual stress becomes smaller with an increase of fibre volume fraction at higher volume fractions. The residual stress at $\theta=0$ changes little when the volume fraction increases from 30 to 40%, whereas a distinct increase of residual stress can be seen when the fibre volume fraction reduces from 20 to 10%. This appears to be consistent with the results obtained in this study, Fig. 3.

It is also noted in the Fig. 3 that the first knee of the 35%SCS-/Ti ß21s is more distinct than that of 1140+/Ti-6-4 composites. Debonding in the SCS-6/Ti ß21s takes place at the carbon/reaction zone interface. The Young's modulus of solution treated Ti ß21s alloy is of ~75 GPa[10], which is significantly lower than the value(115 MPa) of the transverse SCS-6/Ti ß21s composite. Thus a very sharp change of gradient at the first knee can be expected because not only does the composite now contain areas of debonding, but also the modulus of the matrix becomes progressively more important. However in the transverse 35%1140+/Ti-6-4 composite, the Young's modulus is 105±2 MPa[2], which is very similar to the value(106 MPa) of the Ti-6-4 alloy[11]. Therefore any change in gradient now derives from areas of debonding only.

CONCLUSIONS

1. Few AE events can be detected during premature debonding of 1140+/Ti-6-4 composites, whereas in the 35%SCS-6/Ti ß21s composite AE events can be received almost immediately on loading. Bursts of AE events with peak energy were detected in the region of the first knee on stress~time curves. The peak energy of AE events obtained in SCS-6/Ti ß21s is of ~650 µJ, which is approximately three times higher than that obtained in 1140+/Ti-6-4(~150 µJ).
2. A change of fibre volume fraction from 8 to 21% in 1140+/Ti-6-4 shows no effect on the characteristic and distribution of AE events received, however different types of composites(such as SCS-6/Ti ß21s) produce a distinctively different AE results.

ACKNOWLEDGEMENTS

This study is a part of an EPSRC RoPA project. Thanks are also due to the members of the Fatigue and Fracture Group at Birmingham, and particularly to Mr. C. Cooper for help in in situ observations.

REFERENCES

1. Wang, N., Cardona, D.C. and Bowen, P., Int. J. Fract. 75, 1996, pp137-155.
2. Cotterill, P.J. and Bowen, P., J. Mat. Sci., 31, 1996, pp5897-5905.
3. Gundel, D.B., Warrier, S.G. and Miracle, D.B., Acta Mater. Vol.45, No.3, 1997, pp1275-1284.
4. Miracle, D.B., Gundel, D.B. and Warrier, S., "Interfacial Structure and Properties for the Design of Fibre-Reinforced Metal Matrix Composites", published in "Processing and Design Issues in High Temperature Materials", ed. N. S. Stoloff and R.H. Jones, TMS, Warrendale, PA, USA, 1996.
5. Dore, A., Ph.D thesis, "Effects of Fibre Volume Fraction on Tensile Damage and Fatigue Crack Growth in Titanium Metal Matrix Composites", The University of Birmingham, 1997.
6. Liu, J., Ph.D thesis, " Fatigue Crack Growth Resistance and Transverse Tensile Behaviour of a Ti ß21s/SCS-6 Composite", The University of Birmingham, 1997.
7. Wu, X. and Bowen, P., "In Situ Observations of Titanium Metal Matrix Composites under Transverse Tensile Loading-(I)", to be published.
8. Wu, X. and Bowen, P., " In Situ Observations As-processed and Heat Treated TiMMCs under Transverse Tensile Loading-(II)", to submitted.
9. Ding, W., Ph.D thesis, " Medelling and Experimental Studies of Damage in Titanium Metal Matrix Composites", The University of Birmingham, 1997.
10. Fox, K. M., PhD Thesis, "Effects of Interfacial Properties on Fatigue Crack Growth Resistance in Ti/SiC Metal Matrix Composites", 1995.
11. IMI Titanium Ltd., *Titanium Alloy IMI 318*, Manufacturer's technical data sheets.
12. Fanning, J. C., in *Beta Titanium Alloys* in the 1990's, D.Eylon, R.RBoyer, and D.A.Koss, eds, TMS, 1993, pp397-410.